ϕ-meson production at RHIC energies using the upgraded PHENIX detector

October 23, 2005

Research Proposal

Deepali Sharma

Supervisor: Prof. Itzhak Tserruya

Department of Particle Physics

The Weizmann Institute of Science

Rehovot, Israel

Contents

List of Figures

1 Abstract

The ϕ-meson is considered as a diagnostic tool in the quest to understand the Quark Gluon Plasma formed in relativistic heavy-ion collisions as it is particularly sensitive to chiral symmetry restoration and strangeness production. The PHENIX experiment at RHIC has a unique capability to measure the ϕ-meson through both its dielectron and dikaon channels simultaneously, with an excellent mass resolution. A comparison of the ϕ-yields from these two decay channels can reveal important information about modifications in the ϕ-meson properties (mass and/or width) in the medium. This thesis deals with the measurements of ϕ-meson production at RHIC energies using the PHENIX detector upgraded with a novel Hadron Blind Detector which is expected to significantly improve this measurement.

2 Quark Gluon Plasma

Nuclear Collisions serve as a tool to study matter under extreme conditions and as a time machine to study the primordial universe. The current goal of relativistic heavy ion collisions is to produce matter where the quarks effectively decouple from nucleons and behave as quasi-free particles. This state of matter called the Quark Gluon Plasma(QGP), has not occurred in nature since microseconds after the "Big Bang". The QGP state formed in nuclear collisions is a transient rearrangement of the correlations among quarks and gluons contained in the incident nucleons into a larger but globally still color neutral system. This state of nuclear matter is predicted by Quantum Chromodynamics(QCD), the theory of colored interactions which attempts to incorporate all the experimental properties of quarks and gluons even though these particles have never been observed as free particles because of the confining property of the physical QCD vacuum.

Asymptotic freedom[1, 2] and confinement are the two main features of QCD. Asymptotic freedom refers to the weakness of the interaction at short-distance. At small distances, or large momentum transfer (Q^2), the strong coupling constant, $\alpha_s \to 0$. Hence quarks and gluons are weakly coupled and pQCD (perturbative QCD) calculations are justified. On the other hand, at large distances or small momenta, the effective coupling becomes strong resulting in the phenomenon of quark confinement.

The only known method to compute from first principles QCD predictions in the non-perturbative regime is by simulation of lattice Gauge theory. At a critical temperature $T_c \sim$ 155-175 MeV, corresponding to a critical energy density $\epsilon_c \sim 1$ GeV/c^2, lattice QCD predicts a phase transition to a deconfined phase of quarks and gluons where the quark confinement is broken and the approximate chiral symmetry of QCD is restored. This state of matter can be achieved by heating up the system at zero net baryon density (i.e total baryon number equal to zero or in other words the amount of matter and antimatter is approximately equal) to $T_c \approx 170$MeV and/or compressing the cold nuclear matter to baryon densities of about $\rho_c \sim$ 3-10 ρ_0 (where $\rho_0 = 0.15\ fm^-3$ denotes the ground density of nuclear matter). Whether color deconfinement and chiral symmetry restoration are two distinct phase transitions or one, is still in debate, but in any case both phenomena are predicted to occur at similar conditions. The order of the phase transition is also uncertain and depends upon the number of light quark flavors. QCD predicts a second order phase transition in the case of two light quarks, while for three flavors, the transition is of first order.

The predicted QGP and its phase transition to hadronic matter can be realized in the laboratory

by colliding high energy heavy nuclear ions. However after the possible phase transition to QGP, if it exists, the system will quickly expand, cool below the critical temperature T_c so that the hadrons are formed and at freeze-out, they decouple from the fire-ball. The size and lifetime of the plasma are expected to be a few fm in diameter and 10 fm/c in duration. The signals of the QGP have to compete with the background from hot hadronic phase that follows the hadronization of the plasma. Furthermore they could get modified by final state interactions. All this makes the search for the QGP a challenging one.

3 Chiral Symmetry Restoration (CSR)

In addition to the transition to a deconfined state of quarks and gluons, lattice QCD calculations also predict a phase transition associated with the restoration of chiral symmetry which is spontaneously broken at T=0. Quarks like the more familiar photons, have an intrinsic spin and hence chirality associated with them. In the limit of massless particles, chirality is conserved i.e. the number of left-handed quarks or right-handed quarks is a conserved quantity. In the physical world, chiral symmetry is explicitly broken since the quarks have mass. However, for the light quarks, u and d, their current masses are so small (m_u, $m_d \approx$ 5-10 MeV) that chiral symmetry is a very good approximation. But, the interactions among quarks, lead to the spontaneous breaking of the symmetry and only the total number of quarks is conserved. The vacuum expectation value for a quark-antiquark pair is not zero even for vanishing quark masses.

$$< 0|\overline{\psi}\psi|0 > = < \overline{\psi}\psi > \neq 0 \tag{1}$$

The QCD vacuum at any given time contains a certain number of chiral condensates i.e. $q\overline{q}$ pairs that can interact with a (massless) quark traversing the vacuum and hence change its helicity, as if it has mass. This is most likely the origin of the *constituent* quark masses, which are two orders of magnitude larger compared to the *current* quark masses derived for asymptotically free quarks.

In the limit of sufficiently high temperature or density, the chiral condensate drops to zero and consequently the chiral symmetry is expected to be restored. The current lattice QCD calculations show that the transition to a chirally symmetric phase takes place at the same temperature as deconfinement.

3.1 Electromagnetic probes

Electromagnetic probes i.e. dileptons and photons are excellent probes of the early stage of nuclear collisions. They have a relatively large mean free path and so leave the interaction region without any final state interaction, carrying information about the conditions and properties of the matter at the time of their production and in particular of the early stages of the collision. Moreover, they are produced throughout all stages of the collision, and can provide a direct measure of the evolution of the fireball.

A prominent topic of interest is the identification of the thermal radiation emitted from the collision system which could tell us whether the matter formed is the conjectured quark-gluon plasma (QGP) or a high density hadron gas (HG). The elementary processes involved are QCD Compton scattering ($qg \rightarrow q\gamma$) and $q\overline{q}$ annihilation ($q\overline{q} \rightarrow \gamma^* \rightarrow e^+e^-$) in QGP phase and pion annihilation ($\pi^+\pi^- \rightarrow$

$\rho \rightarrow e^+e^-$) in the dense hadron gas. Dileptons originating from $\pi^+\pi^-$ annihilation have a threshold at $2m_\pi$ and a broad peak around the mass of ρ-meson, which dictates the shape of the HG thermal yield. On the other hand, the thermal radiation from QGP has a spectral shape which is essentially an exponential and provides a direct measurement of the plasma temperature. The unambiguous identification of the thermal radiation from QGP is considered as a very strong signal of deconfinement. In practice the measurements are extremely challenging as the thermal radiation is expected to be a small signal in comparison to the large background from competing processes, hadron decays for real photons and Dalitz decays, and γ-conversions for dileptons. Theoretical calculations indicate that the transverse momentum range p_t = 1 - 3 GeV/c is the most promising window where the thermal radiation from the QGP could dominate over other contributions from partonic and hadronic processes in central Au+Au collisions at $\sqrt{S_{NN}}$ = 200 GeV[8].

In addition to the thermal radiation, lepton pairs from hadronic sources in the invariant-mass range $0.5 \leq m_{e^+e^-} \leq 1$ GeV are considered the best probes for chiral symmetry restoration[5]. The study of dileptons allow the measurement of the ρ, ω and ϕ mesons via their dilepton decay channel. An interesting and unique example is that of ρ-meson. Due to its small lifetime (1.3 fm/c) compared to the fireball lifetime formed, most of the ρ-mesons produced in the collision will decay inside the interaction region with modified mass and/or width which might be linked to chiral symmetry restoration. Another interesting vector meson that has acquired lot of attention in recent years is the ϕ-meson. It stands as a unique probe to chiral symmetry restoration in strange sector due to the weakness of the conventional ϕN interaction. As a result its properties are not modified by many body interactions with the surrounding nucleons, thus retaining the information on the condition of initial plasma. The usefulness of ϕ-meson as a probe to hot and dense matter in high energy heavy-ion collisions is discussed in the following section.

3.2 The ϕ-meson

The mass, width and principal decay modes in hadronic and leptonic channels of the ϕ-meson are given in table 1. The K^+K^- decay channel is dominant among the hadronic decay channels.

Quantum Number	$I^G(J^{PC}) = 0^-(1^{--})$
Mass	$1019.456 \pm 0.020 MeV/c^2$
Width	$4.26 \pm 0.05 MeV$
Decay Mode	**Branching ratio**
$\phi \rightarrow K^+K^-$	$(49.1 \pm 0.6)\%$
$\phi \rightarrow K_0^+K_0^-$	$(34.0 \pm 0.5)\%$
$\phi \rightarrow \rho\pi + 3\pi$	$(15.4 \pm 0.5)\%$
$\phi \rightarrow e^+e^-$	$(2.98 \pm 0.04) \times 10^{-4}\%$
$\phi \rightarrow \mu^+\mu^-$	$(2.85 \pm 0.19) \times 10^{-4}\%$

Table 1: ϕ-Meson properties

As discussed earlier, the chiral symmetry restoration may lead to in-medium modifications of the spectral shape (mass and/or width) [5] of the ϕ-meson. The ϕ-mesons because of their longer life time ($\tau \sim$ 40fm/c) predominately decay outside the medium after regaining their vacuum properties, with

only a small fraction decaying inside the hot and dense fireball. Since the measurements are integrated over the whole collision history, small modifications are expected in the ϕ-meson line shape manifesting themselves predominately as a tail at lower masses. An excellent mass resolution is needed to identify these effects. The ϕ-meson offers also unique capabilities to study in-medium effects through the simultaneous measurement of its decay into K^+K^- and e^+e^-. Since the mass of the ϕ-meson is very close to twice the kaon mass ($m_\phi - 2m_K = 0.032$ GeV), its width in free space is small (about 4.26 MeV). In the nuclear medium, both kaon and phi meson masses may change. If the decrease of $m^*_K + m^*_{\overline{K}}$ is larger than that of m^*_ϕ, then the ϕ-meson decay width would increase, leading to a broader ϕ-meson mass spectrum. In addition to that, a strong decrease of the ϕ-meson mass may have a strong effect in the branching ratio of the $\phi \rightarrow K^+K^-$ decay channel. But the interpretation might not be simple because the scattering and absorption of low-momentum kaons in the medium may also lead to a small ϕ-meson yield in this decay channel. A precise comparison of the yields and line-shape in the two decay channels will provide a powerful diagnostic tool.

In addition to the above properties, the ϕ-meson is of further interest because it is the lightest vector meson with hidden strangeness $s\overline{s}$ content making it sensitive to strangeness production. An enhancement of ϕ-meson has been suggested as a possible signature of deconfinement since in a QGP, the copious production of s and $\overline{s}$ originating from annihilation of gluons ($g + \overline{g} \rightarrow s + \overline{s}$) and light quarks and anti-quarks ($u(ord) + \overline{u}(ord) \rightarrow s + \overline{s}$), would very likely lead to formation of ϕ-meson during the hadronization phase. While in normal hadronic interactions, the production of ϕ-meson is OZI[6] suppressed according to which strong interaction processes where the final state can only be reached through quark, anti-quark annihilation are suppressed. Furthermore, the ϕ-meson interacts weakly with non-strange hadrons and so keeps information about the early stages of the colliding system and reaction dynamics.

4 Results from experiments at SPS energies

At the CERN SPS, the ϕ-meson production in central collisions at 158 AGeV has been studied via the muon decay channel by NA50 (Pb+Pb)[9] and via the kaon decay channel by NA49 (Pb+Pb)[10] and CERES (Pb +Au). But the information about the ϕ-meson from these experiments is inconclusive. The NA50 experiment observed a significant increase of the $\phi/(\rho + \omega)$ ratio with centrality which is attributed to an enhancement of the ϕ-production. The NA49 experiment found an increase of the ϕ/π ratio which is also attributed to an enhancement of the ϕ production. However, the inverse slope parameters T, as obtained from an exponential fit to the ϕ-m_T distributions are T=218±10 MeV, 283±11 MeV and 305±15 MeV in the NA50, CERES and NA49 experiments, respectively. There is an even larger discrepancy in their measured ϕ-yields[14]. The NA50 yields are larger than those of NA49 by factors of 2 to 4 in the common m_T range covered by the two experiments (see fig. 1(b). It is unclear whether these differences are of experimental origin or a manifestation of in-medium effects. Additional insight on this issue is provided by the first NA60 results from In+In collisions at 158 AGeV. Fig. 1(a) shows the multiplicity dependence of the inverse slopes i.e temperature calculated by NA60 from its dimuon data plotted together with the slopes calculated by NA49 (Pb-Pb) using $\phi \rightarrow K^+K^-$ and those from NA50 (Pb-Pb) using $\phi \rightarrow \mu^+\mu^-$. The temperature parameter T measured by NA60 and NA49 are in agreement with each other and show a clear rise with centrality, whereas NA50 results are consistent with a flat distribution[15]. On the other hand, the NA60 ϕ/ω ratio is in

very good agreement with the NA50 results.

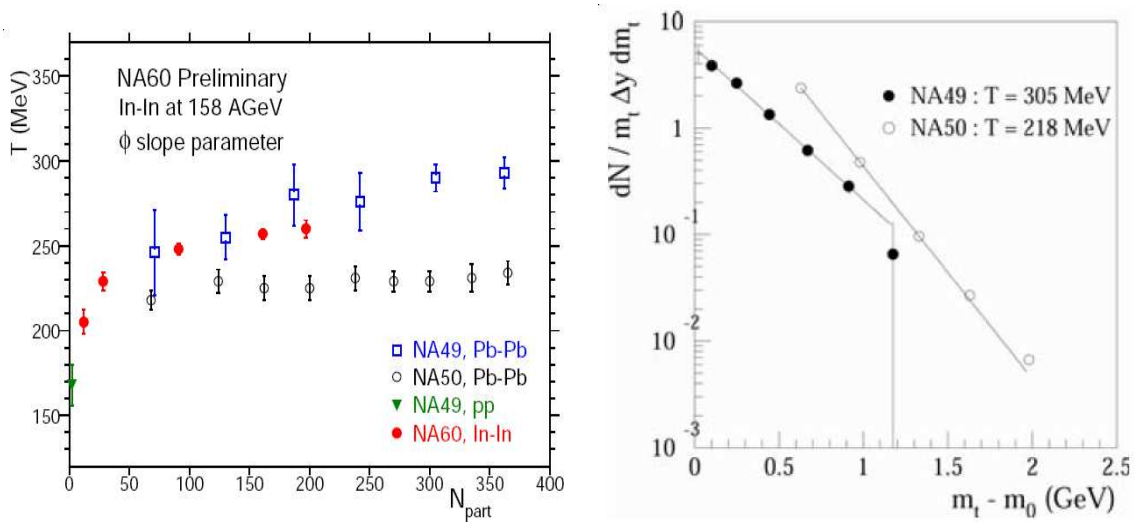

(a) (b)

Figure 1: The left panel shows the ϕ m_T inverse slope parameter T[15] for different experiments at 158 GeV/nucleon. NA50 points from the window $m_T > 1.5$ GeV are converted to $p_t > 1.1$ GeV using T = 228 MeV measured by NA50 for the extrapolation. The right panel shows the ϕ-m_T spectra for NA49 And NA50.

Results from first measurements of the ϕ-meson production at RHIC are already available. A detailed description of the present status of the ϕ-meson analysis achieved with PHENIX is discussed in section 4.2.

5 The PHENIX experiment at RHIC

The Relativistic Heavy Ion Collider at the Brookhaven National Laboratory is a versatile machine able to accelerate a wide variety of nuclei up to 100 GeV per nucleon and protons up to 250 GeV. RHIC's main physics mission is to collide heavy ions to study nuclear matter under extreme conditions. RHIC started operation in the year 2000 colliding gold nuclei at a center of mass energy of $\sqrt{S_{NN}} = 130$ GeV and has completed five successful physics runs since then. PHENIX (Pioneering High Energy Nuclear Interaction Experiment)[16] is one of the largest of four experiments running at RHIC. The others being STAR, PHOBOS and BRAHMS.

PHENIX is a sophisticated multi-detector system designed to measure hadrons, leptons and photons with excellent momentum and energy resolution. The variety of sub-detectors within PHENIX experiment allows the possibility to explore the initial stages of hot matter formed in heavy-ion collisions as well as cold nuclear matter in d+Au collisions.

5.1 The PHENIX detector

The PHENIX detector subsystems are grouped into four spectrometers: two Central arms around mid rapidity that cover $|\eta| < 0.35$ ($70° < \theta < 110°$) and 90° in azimuth φ and two Muon arms covering $1.1 < |\eta| < 2.4$ (South) or $1.2 < |\eta| < 2.4$ (North) with full 2π coverage in φ - and a set of global detectors. The global detectors comprising of Silicon Vertex Detector, Beam Beam Counters and

Zero Degree Calorimeters measure the time and position of the interactions, and the multiplicity of produced particles.

The Central arms of PHENIX consist of elements that perform particle tracking, momentum measurements, electron, photon and charged particle identification. They contain a Central Magnet that provides an axial magnetic field (field integral ≈ 0.78 T·m) parallel to the beam in the interaction region. The charged particle tracking is provided by Drift Chambers and Pad Chambers. The Drift Chambers (DC) are located in both arms between 2.0 to 2.4 meters from the beam direction and determine p_t by measuring the charged particle trajectories in the $r - \varphi$ plane, as they curve in the axial magnetic field produced by the central magnets. The measured single particle momentum resolution at the DC is 0.5% between 200 MeV/c and 1GeV/c. The Pad Chambers aid the tracking by providing a 3-dimensional space point measurements of the particle tracks.

Particle identification is achieved by combining information from several detectors. These consist of a high resolution Time of Flight (TOF) detector, two types of Electromagnetic Calorimeters (EMCals): one made of lead-glass (PbGl) and the other of lead and scintillator material (PbSC), and a gas filled Ring Imaging Čerenkov (RICH) detector. The TOF located in the east arm only, together with the EMCals provide PHENIX with an excellent hadron identification capability over a momentum range of $0.3 < p < 2.5$ GeV/c. Electrons are identified with the RICH and the EMCal as described in next section.

Fig. 2 shows an overall layout of the PHENIX detector as used in Run 4.

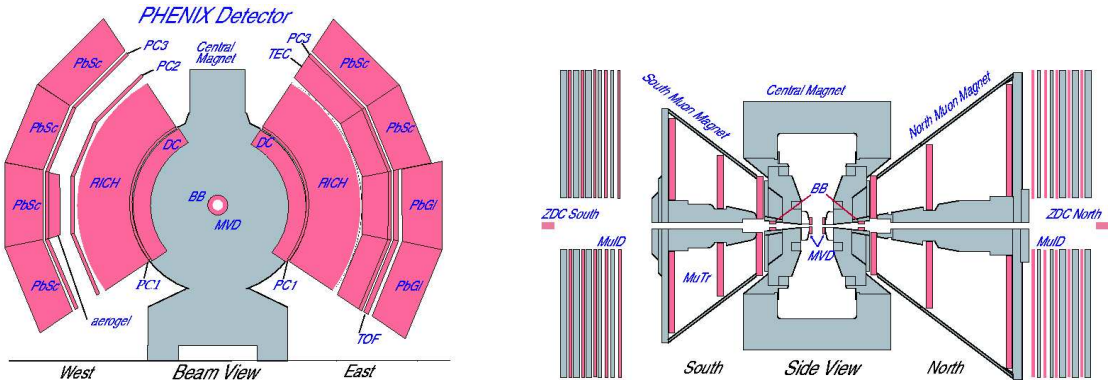

(a) (b)

Figure 2: PHENIX detector configuration used in Run 4

5.2 ϕ meson with the present PHENIX set up

With its excellent mass resolution, the PHENIX detector has the potential to perform the precision spectroscopy of ρ, ω and ϕ meson. PHENIX can measure the ϕ meson through both its K^+K^- and e^+e^- decay channels simultaneously. The kaons identification is achieved using the high resolution TOF and the EMCals. The TOF provides π/K separation for $0.3 < p < 2.5$ GeV/c, with a timing resolution of about 120 ps and the EMCal provides π/K separation for $0.3 < p < 1.0$ GeV/c with a timing resolution of about 480 ps.

The electrons are identified using the RICH and EMCal detectors in the p_t range of 0.2 to 5 GeV/c. RICH is a threshold CO_2 gas Čerenkov detector, with a thin mirror that reflects the Čerenkov light onto photo-multipliers located outside the spectrometer acceptance. Due to the different thresholds

for electrons and pions to generate Čerenkov light, the RICH provides a good separation of the two species. The second detector in electron identification is the EMCal. An electron passing through the EMCal deposits most of its energy while a hadron has a large probability to deposit only a small fraction of its energy and hence requiring the energy to match momentum (E/p $\approx$ 1) provides electron identification.

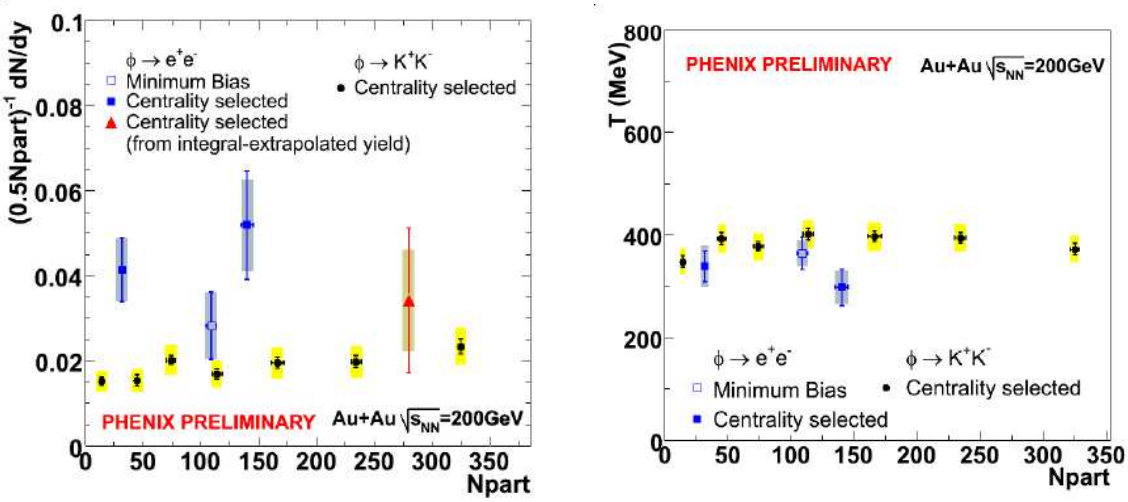

(a) (b)

Figure 3: Multiplicity dependence of the yield dN/dy (left panel) and temperature T (right panel) for e^+e^- and K^+K^- decay channels. Open and filled symbols represent minimum bias and centrality selected points. Squares are for $\phi \rightarrow e^+e^-$ and circles represent $\phi \rightarrow K^+K^-$ points. The triangle represents $\phi \rightarrow e^+e^-$ yield derived by some different analysis[12]

An analysis of the ϕ-meson production through the K^+K^- and e^+e^- decay channels has been attempted by PHENIX[11, 12]. The K^+K^- decay channel has been studied thoroughly, but the measurements in dielectron channel suffer from severe limitations. A comparison of the yields (dN/dy) and temperature parameter (T) as extracted from the two decay channels with the present PHENIX set up is shown in Fig. 3. The temperatures (right panel) measured in the two decay channels seem to be in agreement with each other within errors and do not show any centrality dependence. The rapidity density per participant pair ((dN/dy)/(0.5·N_{part})) appears also to be independent of centrality but the dN/dy value in the e^+e^- channel seem to be larger than that in K^+K^- channel. However, the e^+e^- decay channel has too large error bars, both systematic and statistical preventing us from making a precise comparison with the dikaon channel. The reason for the large error bars in e^+e^- channel is the huge combinatorial background produced by the uncorrelated pairs from π^0-Dalitz decay and γ-conversions. This arises from the fact that the PHENIX detector with its present configuration has a limited angular acceptance in the central arms and a strong magnetic field beginning radially at R=0. As a result, low momentum tracks can not leave the magnetic field region and very often only one track from the pairs coming from π^0-Dalitz decays and γ-conversions is detected thus producing an overwhelming combinatorial background. Moreover, the signal from hadronic sources is expected to be proportional to the number of charged tracks N_{ch}, while the combinatorial background increases quadratically with N_{ch}. Since the signal is obtained by subtracting the combinatorial background, this very poor S/B ratio implies a very large statistical as well as systematic uncertainty making the significance of the signal very limited.

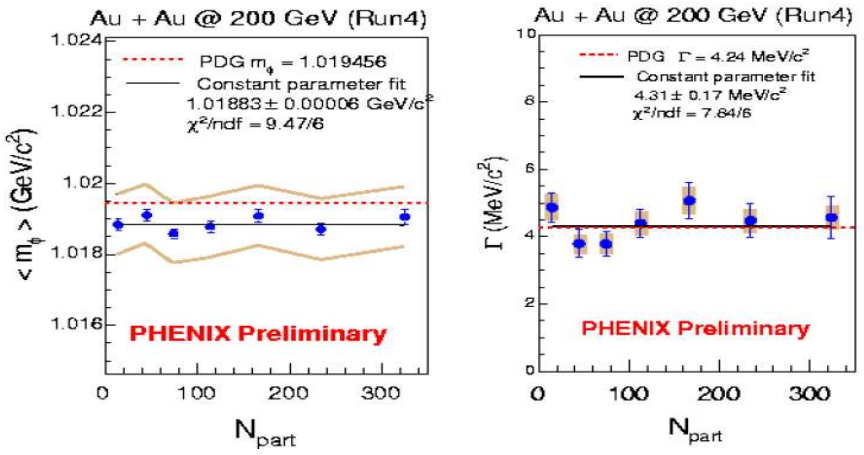

Figure 4: Centrality dependence of line shape

In the run 4 measurement of the ϕ-meson decay to e^+e^- pairs, the S/B is $\approx 1/53$. On the other hand the S/B is $\approx 1/10$ in the K^+K^- decay channel. The much higher statistics and better S/B ratio in this case allowed us to perform a line shape analysis of the ϕ-meson. The results showed no significant change in the centroid and width values of the ϕ-meson from the PDG accepted values as can be seen in the Fig. 4. However, such a study in the e^+e^--decay channel could not be carried out owing to the limited significance of the result and the large combinatorial background as explained above. But a considerable improvement in the e^+e^- channel is expected with the planned upgrade of the PHENIX detector with a novel Hadron Blind Detector which is expected to significantly reduce the combinatorial background.

5.3 Upgrade of the PHENIX detector: Hadron Blind Detector

As discussed in previous section, inspite of the excellent electron identification capability of PHENIX, the present set-up lacks the ability to reject the overwhelming combinatorial background coming from π^0-Dalitz decays and γ-conversions making the measurement of low-mass electron pair continuum practically impossible. An HBD has been developed by the Weizmann Institute group as an upgrade of the PHENIX detector. The main task of the HBD is to recognize and reject tracks originating from π^0-Dalitz decays and γ-conversions thus allowing to measure low mass ($m_{e^+e^-} \leq 1$ GeV/c^2) electron-positron pairs produced in central Au + Au collisions at RHIC energies. The main idea is to exploit the fact that the opening angle of electron pairs from these sources is very small compared to pairs from vector mesons. The HBD is therefore located in a field-free region where the pair opening angle is preserved. The field free region is created by an inner coil, recently installed in the central arms of PHENIX. This coil counteracts the main field of the outer coils and creates an almost field-free region close to the vertex and extending to $\approx$ 50-60 cm in the radial direction (Fig. 5(a)).

Conceptual Monte Carlo simulations[17] were done at the ideal detector to quantify the potential benefit and define the system specifications of the HBD. The results of the study indicated that a reduction of the combinatorial background originating from conversions and π^0-Dalitz decays of at least two orders of magnitude can be achieved with a detector that provides electron identification with a very high efficiency, of at least 90% and also a double (electron) hit recognition at a comparable level. A careful consideration of the possible realizations for the HBD led to the following detector

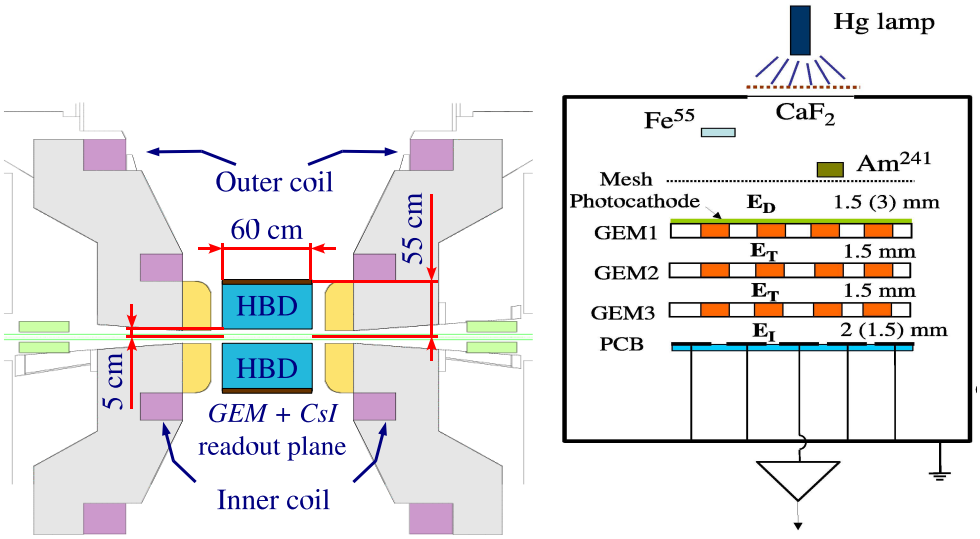

(a) (b)

Figure 5: The left panel shows PHENIX detector together with the proposed HBD location and inner coil and the right panel shows the set-up used for R&D studies.

scheme.

The HBD is a windowless *Čerenkov* detector operated with pure CF_4, in a proximity focus configuration. The detector consists of a 50 cm long radiator directly coupled to a triple GEM detector[18] which has a *CsI* photocathode evaporated on the top face of the first GEM foil and a pad readout at the bottom of the GEM stack. In this scheme the *Čerenkov* light from particles passing through the radiator is directly collected on the photocathode forming a circular blob image rather than a ring as in a RICH detector. Simulations show that with such a detector configuration, an opening angle cut of ∼200mrad, will suppress the combinatorial background by approximately two orders of magnitude while preserving ∼50% of the signal. This scheme offers a number of very attractive features:

- The use of CF_4 both as radiator and detector gas in windowless geometry results in a large bandwidth (from ∼ 6 eV given by the CsI threshold to ∼ 11.5 eV given by the CF_4 cut-off) which eventually leads to a large number of photoelectrons per incident electron. This results in single electron detection efficiency and a double-hit recognition larger than 90%.

- The second feature is that GEMs allow the use of reflective photocathode. The top face of the first GEM is coated with a thin layer of CsI and the photoelectrons are pulled into the holes of the GEM by their strong electric field. In this configuration photon feedback effects are avoided.

- The readout scheme foresees the detection of *Čerenkov* photoelectrons in a pad plane with hexagonal pads of size comparable to the blob size (∼10 cm^2). This leads to a very small probability for a single-pad hit by an electron entering in HBD in comparison to a hadron which will produce a single pad hit with a 100% probability, thus providing a strong handle in the hadron rejection factor of HBD.

- The relatively large pad size results in a low granularity, and hence low cost, detector. In addition, a primary charge of atleast 10 electrons/pad is expected, allowing operation of the

detector at a relatively moderate gain of a few times 10^3. This is a crucial advantage for the stable operation of a UV photon detector.

However, the concept discussed above was new and involved many elements, which had never been tested before in the laboratory and so it required a comprehensive R&D.

5.4 R&D results

The validity of the HBD concept discussed above has been demonstrated in a comprehensive R&D program[19, 20]. The R&D set-up used consisted of a triple GEM detector mounted inside a stainless steel box that can be pumped down to 10^{-6} before gas filling, along with an Fe^{55} source and an ^{241}Am alpha source (see Fig. 5(b). The measurements with UV photons were done with a Hg-lamp. All the measurements were done with GEMs produced at CERN having 50 μm kapton thickness, 5μm thick copper layers , 60-80 μm diameter holes and 140 μm pitch, with a sensitive area of either 3 $\times$ 3 or 10 $\times$ 10 cm^2. In particular, it has been shown that

- A triple GEM detector can operate in a very stable mode with pure CF_4 at gains in excess of 10^4 (Fig. 6(a)).

- A charge saturation effect occurring in CF_4 makes the HBD relatively robust against discharges. The measurements reveal that the limit of stability is dictated by the quality of the GEM foils rather than by the presence of heavily ionizing particles.

- Aging studies of the CsI photocathode as well as GEM foils showed no sizable deterioration of the detector gain and CsI quantum efficiency for irradiation levels of $\sim$150$\mu C/cm^2$ that corresponds to $\sim$10 years of normal PHENIX operation at RHIC.

- The CsI quantum efficiency measurements in CF_4 were done in the range 6-10.3 eV (120-200nm). A linear extrapolation to the expected operational bandwidth of the device (6-11.5 eV) gives a figure of merit $N_0 = 822cm^{-1}$ and $\sim$36 photoelectrons over a 50 cm long radiator.

- Systematic measurements of detector response to electrons, mip's and α-particles as a function of drift field E_D (the field in the gap between the mesh and upper GEM) were done. A slightly reversed field in this gap strongly suppresses the charge collection from this gap while the photo-electrons are effectively collected by the strong field inside the GEM holes as shown in fig. 6(b) and fig.. 6(c). A combination of amplitude response with hit size leads to large hadron rejection factors of $\sim$ 100 with electron detection efficiency larger than 90%.

A test of triple GEM detector was carried out recently, inside the PHENIX central arm spectrometer located at a distance of 50 cm from the collision point and operated with pure CF_4 in the Au + Au collisions[21]. The detector operated smoothly with no discharges or gain instabilities.

The full-scale prototype design has been integrated into the PHENIX standard simulation package (PISA). Realistic simulation studies were performed using central HIJING Au + Au collisions at $\sqrt{S_{NN}}$ = 200 GeV with embedded ϕ-mesons. The results show that for the mass region around ϕ-meson, a reduction by a factor of more than 100, can be achieved in the combinatorial background coming from π^0-Dalitz decays and γ-conversions.

The successful completion of the R&D and the beam test, combined with the results of simulation studies demonstrated the validity of the HBD concept and paved the way for the incorporation of such a detector in the PHENIX experiment. The HBD is now an official PHENIX project[22] with installation and commissioning foreseen in year 2006.

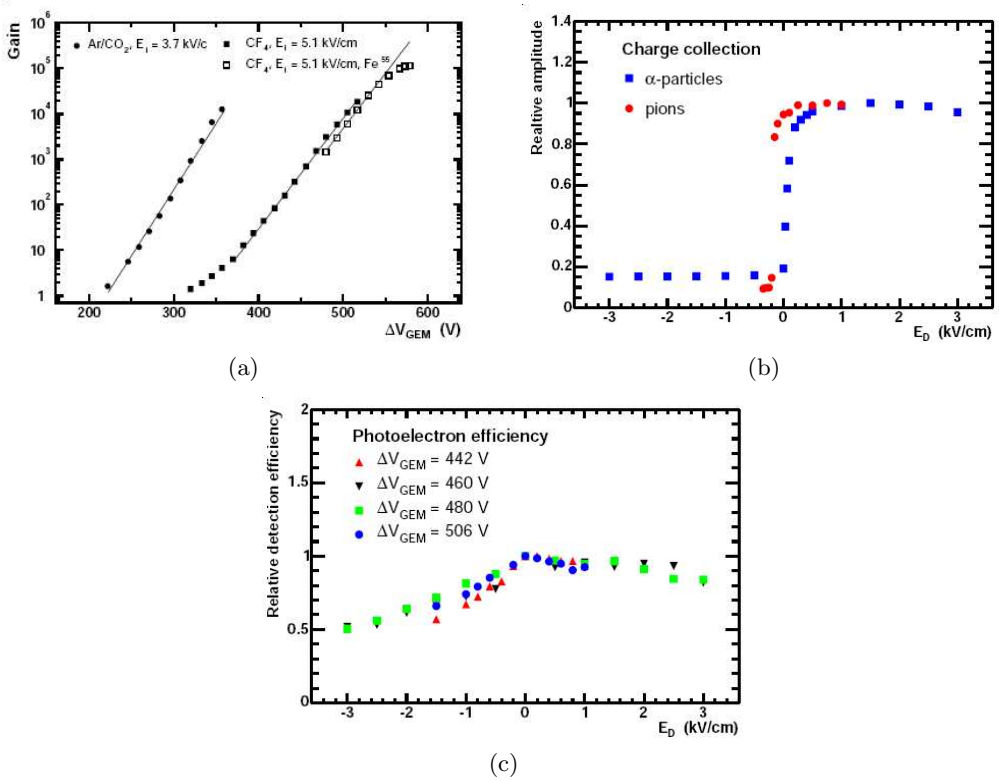

Figure 6: The top left panel shows gain as a function of ΔV_{GEM} for Ar/CO_2 and CF_4 measured with a Hg UV lamp. For CF_4, the gain curve with X-rays from ^{55}Fe is also shown. The lines are exponential fits to the data[19]. The top right panel shows the collection of ionization charge from 1 GeV/c pions and α particles from ^{241}Am vs. the drift field E_D in the gap between the mesh and the upper GEM and the bottom panel shows the photoelectron detection efficiencies for different gains vs electric field E_D[20].

6 Research proposal

My research work will mainly be focused on two parts.

1) I will participate in the construction of the final HBD. A full-scale HBD prototype very close to the final design has been successfully constructed. The HBD is made of two identical arms located close to the interaction vertex (figs. 5(a), 7(a)), with each arm consisting of a $\sim$ 50 cm long radiator directly coupled to a triple GEM photon detector. This configuration gives an extended acceptance (135^0 in azimuth (φ) and ± 0.45 units in pseudorapidity (η)) in comparison to the Central arms thus providing a generous veto area for efficient rejection of close pairs. The detector element in each arm is sub divided in 12 detector modules, 6 along the φ and 2 along the z-axis with module size 23×27 cm^2 as can be seen in Fig. 5. Fig. 7(b) gives an exploded view of HBD panel.

The construction of final HBD has started at the Weizmann Institute of Science. Our group is

responsible for production of GEM panels, that will include gluing and assembling on FR4, test of detector modules, construction of HBD vessels and mounting HV resistors. The final detector assembly and CsI evaporation will be done at Stony Brook University. I will participate in the production of detector components, testing of GEM foils and will work on the first calibrations of GEMs, gain measurements and storing all this information into a database.

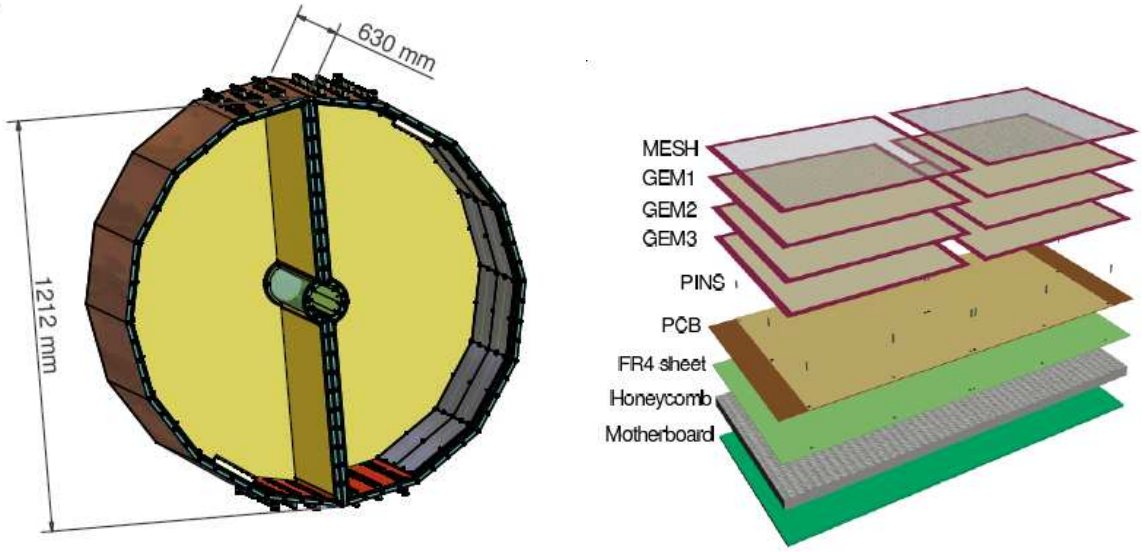

(a) (b)

Figure 7: The left panel shows a 3-d view the HBD final design and the right panel shows an exploded view of one panel of the HBD.

2) On the physics analysis part, I will mainly focus on studying the ϕ-meson production. As discussed earlier in section 2, the ϕ meson provides a diagnostic tool for in-medium modifications of the light vector mesons and chiral symmetry restoration in particular. The strangeness content of ϕ-meson makes it a sensitive probe for strangeness production. In addition to that, the measurements in p + p and d + Au collisions will be essential to establish a baseline for these studies and to understand cold nuclear matter effects. As discussed in section 4.2, the present PHENIX measurements in the e^+e^- decay channel are inconclusive due to a very poor S/B ratio. The quality will get dramatically improved once the HBD is installed. So, the main aim of my research work will be to study the $\phi \rightarrow e^+e^-$ decay channel in Au + Au collisions with the HBD installed. I am presently analyzing the run 5 p + p data taken this year.

References

[1] D.Gross and F.Wilezek, Phys.Rev.Lett.30(1973).

[2] H.Politzer, Phys.Rev.Lett.30(1973).

[3] Yuri L.Dokshitzer. QCD Phenomenology. 2003.hep-ph/0306287.

[4] A.J. Baltz and C. Dover. Phys. Rev., C53:362, 1996.

[5] S. Pal, C.M. Ko and Z. Lin, Nucl. Phys. A707, (2002) 525

[6] S.Okuba, Phys. Lett. 5 (1963) 165; J. Iizuka, Prog. Theo. Phys. Suppl. 37-38 (1966) 21.

[7] R. Rapp, nucl.th/0204003 (2002).

[8] S. Turbide, R. Rapp and C. Gale, Phys. Rev. C69,(2004)

[9] B. Alessandro et al., Phys. Lett. B555 (2003) 147.

[10] S.V. Afanasiev et al., Phys. Lett. B491 (2000) 59.

[11] D. Mukhopadhyay for the PHENIX Collaboration, Nucl. Phys. A715, 494c(2003).

[12] A.Kozlov for PHENIX collaboration, see Proceedings QM'05

[13] M. Masera, Nucl. Phys. A590 (1995) 93c.

[14] J. Phys. G: Nucl. Part. Phys. 27(2001) 355-366.

[15] First results from NA60 on low mass muon pair production in In-In collisions at 158 GeV/nucleon, J.Phys. G31 (2005) S903-S910. Study of dimuon production in Indium-Indium collisions with the NA60 experiment arxiv:hep-ex/0505049 v2.

[16] The PHENIX EXPERIMENT AT RHIC, Nucl. Phys. A638, 565(1998), D.P.Morroson et al,. Archive: hep-ex/9804004.

[17] PHENIX Technical Note 391: Proposal for a Hadron Blind Detector, 2001.

[18] F. Sauli, Nucl. Instr. and Meth. A 386 (1997)531.

[19] NIM A523, 345, 2004.

[20] NIM A546, 466, 2005.

[21] B.Azmoun, N.Smirnov, S.P. Stoll, C.L. Woody, Paper

[22] PHENIX Technical Note 415, Conceptual Design Report on a HBD Upgrade for the PHENIX Detector. N16-49, IEEE, Rome 2004.